Preparation of phosphorylated conjugated microporous organic polymers and extraction of low-concentration rare earth elements

Zhiqian Liu[1,2], Yace Mi[1,a], Qing Liu[2], Meng Rong[2,b], Liangrong Yang[2,c]

[1] College of Chemical Engineering, Inner Mongolia University of Technology, Hohhot, 010051, China
[2] CAS Key Laboratory of Green Process and Engineering, Institute of Process Engineering, Chinese Academy of Sciences, Beijing 100190, China

Abstract. Aiming at the extraction and recovery of rare earth elements (REEs) in low-concentration rare earth leaching tailings, a kind of phosphorylated conjugated microporous organic polymer (P-CMP) was prepared and applied to adsorb rare earth ions (Nd^{3+}, Dy^{3+}, Y^{3+}). The structure of P-CMP was characterized by FT-IR. SEM and EDS were utilized to illustrate the surface morphology and element distribution of P-CMP, respectively.The adsorption mechanism of P-CMP was determined by XPS. The effects of pH, ion concentration and adsorption time on adsorption capacity were investigated. The isotherm of the rare earth adsorption process was fitted by Langmuir and Freundlich models, and the kinetics was fitted by Pseudo-first-order and Pseudo-second-order. The results show that P-CMP is an amorphous microporous material, which has strong interaction with Nd^{3+} (30.18 mg/g), Dy^{3+} (37.84 mg/g) and Y^{3+} (22.01 mg/g), and the synergistic effect of amino and phosphate groups provides good selectivity (S.F.(Nd^{3+}/Me^{n+}) = $5*10^3$~$5*10^4$). The P-CMP selectively adsorbs rare earth ions in the actual system and cycles 8 times.

1. Introduction

Rare earth has always been known as an industrial vitamin, because of its special magnetic, optical, electrical properties, which is widely used in aerospace, information manufacturing, green energy, biochemistry and other fields [1]. The need of rare earth elements has elevated due to the industry developing rapidly, and the waste of rare earth leaching tailings is serious [2]. The content of rare earth in leaching tailings is low along with high-concentration impurity ions (Al^{3+}, Ca^{2+}, Mg^{2+}, Mn^{2+}, K^{+}, Na^{+}), thereby difficult to make secondary utilization [3].

At present, the separation methods of rare earth ions mainly include precipitation, extraction, membrane separation and adsorption, among which the adsorption stands out of economical utilization and stable cycle performance [4], and is more suitable for rare earth tail liquid with low concentration and high interference ions. The types of adsorbents encompass porous organic polymers, inorganic materials, and cost-effective biomaterials [5]. There are many kinds of porous organic polymers, with high adjustable degree, stable adsorption performance and low cost, but the traditional porous polymers have disadvantages of low adsorption capacity, slow kinetics and poor selectivity [6]. Conjugated microporous polymers prepared by coupling reaction have low monomer requirements and high crosslinking degree, providing a method for introducing functional groups [7].

Most adsorbents introduce a high density of single functional groups. Although the adsorption capacity of the adsorbents is pretty high, it is unsatisfying for their indistinguishable adsorption and sluggish kinetics. In this work, the synergistic action of phosphoric acid and amino group was introduced to adsorb rare earth ions, leading to enhancing the kinetics and selectivity to interfering ions [8-9].

2. Preparation and characterization

2.1 Preparation of materials

Firstly, by Knoevenagel condensation reaction, the conjugated microporous polymer with double bond was formed by pyroquinol and p-phenyldiformaldehyde under the condition of catalyzing by dimethylamine. Secondly, the cyano-rich polymer was subsequently subjected to modification in phosphorous acid at a temperature of 80 °C. The initial cyanide group was replaced by a secondary amino group and two phosphate groups, following by washing and drying, and then a powder adsorbent with dark red was formed for use. As shown in Fig 1.

Corresponding author's e-mail: miyacetx@163.com[a], mrong@ipe.ac.cn[b], lryang@ipe.ac.cn[c]

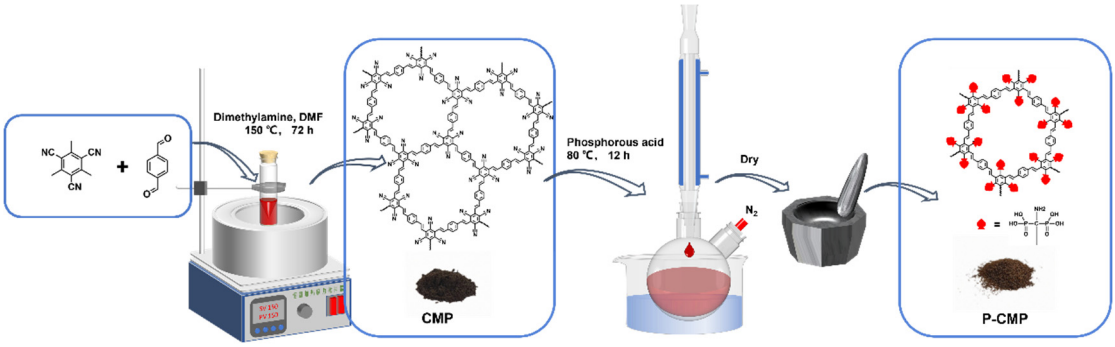

Figure 1. Synthesis route of P-CMP.

2.2 Characterization

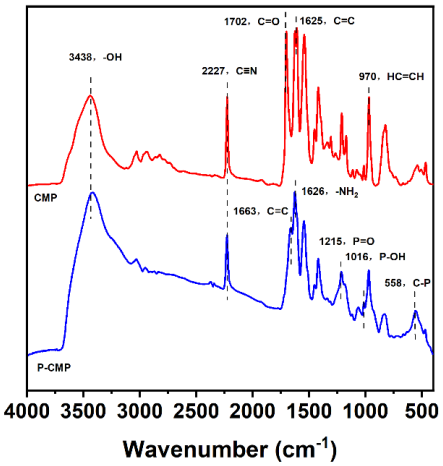

Figure 2. Fourier transform infrared spectra of P-CMP

The materials before and after modification were characterized by Fourier infrared spectroscopy (Fig 2). Because of the transformation from C≡N to -NH_2, the vibration peak of C≡N corresponding to 2227 cm^{-1} had a significant decrease, and the characteristic peak of secondary amino group appeared at 1626 cm^{-1}. A new tensile vibration peak observed at 558 cm^{-1} was speculated to C-P bind, signifying the successfully grafting phosphoric acid groups onto the conjugated microporous skeleton surface. The stretching vibration peaks of P=O and P-OH at 1215 cm^{-1} and 1016 cm^{-1} were also observed from FTIR spectra.

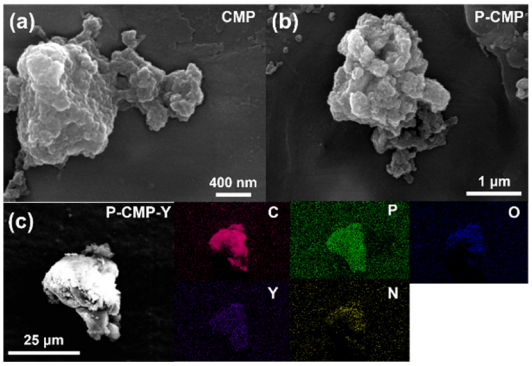

Figure 3. SEM images of CMP (a) and P-CMP (b); (c) Elemental mappings of P-CMP after adsorption loading Y^{3+}

The surface morphology was characterized by scanning electron microscopy along with energy dispersion spectrometer for element distribution of the adsorbent. As shown in Fig 3, the surface of the adsorbent was displayed as compact agglomeration of irregular spheroids with diameters changing between 40 to 86 nm, The morphology of raw materials did not change after phosphorylation. which indicated that the material belonged to amorphous polymer. According to Fig 3c, the adsorbent was composed of C, O, P and N elements, and loaded with a large amount of Y^{3+} proving that P-CMP was successfully prepared and had good an adsorption effect on rare earth ions.

3. Adsorption experiment

3.1 pH effects

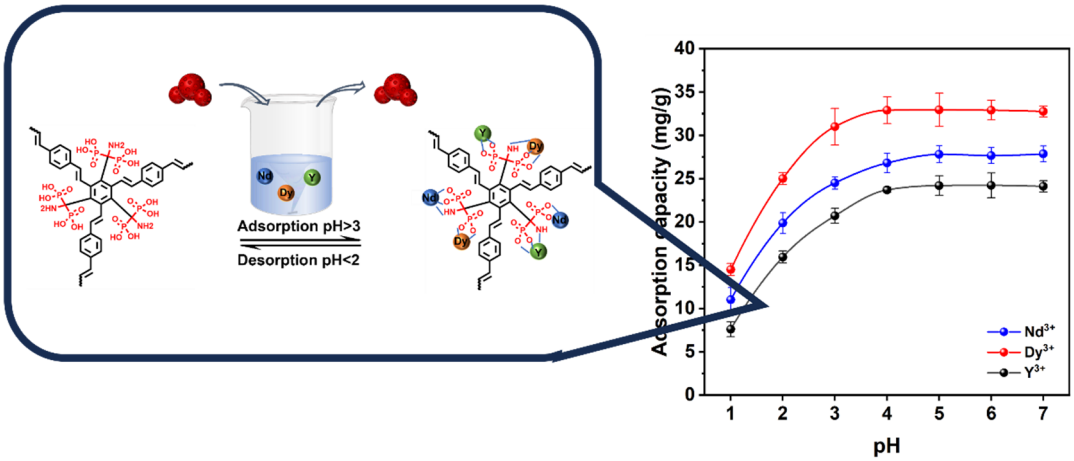

Figure 4. Effect of pH on Nd^{3+} adsorption of P-CMP ($C_{0(REE^{3+})}$=200 ppm, T=298 K, S/L=1 g/L, 24 h)

From Fig. 4, it can be concluded that the application of P-CMP had a wide pH range: the adsorption of rare earth ions was stable in the range of 23-35 mg/g at pH>2. All adsorption sites in this range can electrostatically interact with rare earth ions. When the pH continued to decrease (pH<2), H^+ in the solution will compete with rare earth ions for adsorption sites, leading to protonation of the adsorption site, which carried a positive charge to repel rare earth ions. Such investigation also proved the probability of rare earth ions desorption after adsorbing.

3.2 Isotherms and dynamics

Table 1. Fitting data of the adsorption isotherm of P-CMP.

REEs	Langmuir			Freundlich		
	Q_m(mg/g)	K_L(L/mg)	R^2	n	K_F ($mg^{1-n}L^n/g$)	R^2
Nd	30.18	8.163	0.991	19.89	22.04	0.909
Dy	37.84	6.127	0.994	14.43	23.57	0.990
Y	22.01	4.041	0.995	14.74	13.84	0.701

Table 2. Kinetic fitting parameters.

REEs	Pseudo-first-order			Pseudo-second-order		
	Q_e(mg/g)	K_1(min^{-1})	R^2	Q_e(mg/g)	K_2($g/mg^{-1}\cdot min^{-1}$)	R^2
Nd	29.79	0.445	0.996	30.76	0.0322	0.998
Dy	38.11	0.523	0.995	39.14	0.0334	0.999
Y	21.27	0.247	0.988	63.17	0.0027	0.991

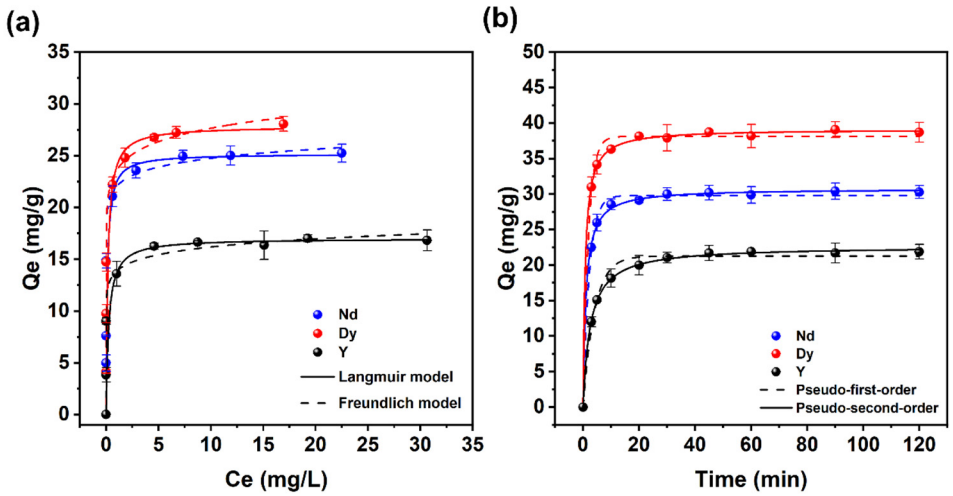

Figure 5. (a) Adsorption isotherms of P-CMP (pH = 4, T=298 K, S/L=1 g/L, 24 h); (b) Effect of contact time on REE^{3+} adsorption capacity of PO-PPR-1 ($C_{o\ (REE^{3+})}$=200 ppm, T=298 K, pH=4, S/L=1 g/L).

3.2.1 Isotherm model

P-CMP was used to perform isotherm tests for Nd^{3+}, Dy^{3+} and Y^{3+} respectively, and the rare earth solution concentration was 5-50 ppm. The Langmuir model and Freundlich model were explored to fit the data and the results were shown in Fig. 5a. The adsorption capacity augmented with the increase of the initial concentration and finally stabilized to 20-30 mg/g. The adsorption capacity of P-CMP for three rare earth ions followed the order of Nd^{3+} < Dy^{3+} < Y^{3+} (mole), which is consistent with the general rule that heavy rare earth elements have a higher affinity for phosphate ester adsorbents. Details of the fitting results were shown in Table 1. It can be clearly seen that the adsorption process is more consistent with the langmuir adsorption model, which signifies that the adsorption process is a single layer adsorption, and the adsorption sites are uniformly distributed on the surface of the adsorbent without interference.

3.2.2 Dynamic model

The pseudo-first-order kinetic equation and pseudo-second-order kinetic equation were carried out kinetic fitting of the P-CMP adsorption rate of rare earth ions, and the fitting results were shown in Figure 5b. The adsorption capacity increased with the increase of adsorption time, and did not change at 20min, meaning that P-CMP had a fast adsorption rate for rare earth ions, and reached adsorption equilibrium within 20 min. Referring to Table 2 for details of the fit: the value of Qe obtained from the pseudo-second-order dynamics coms near Qm, and R^2 is higher than the other's model, indicating that the adsorption process belongs to chemisorption.

3.3 Selectivity

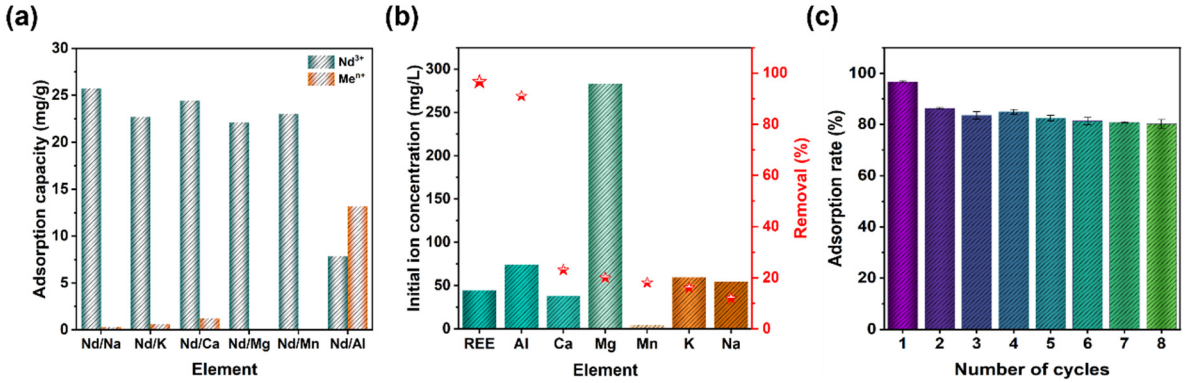

Figure 6. (a) Adsorption capacity of P-CMP for Nd^{3+} in two-element system ($C_{o\ (REE^{3+})}$=50 ppm, Nd^{3+}: Me^{n+}=1:5 (mole), S/L=2 g/L, T=298 K, 24 h, pH=4); (b) Selective adsorption of P-CMP in real tail liquid (S/L=10g/L, T=298K, 24 h, pH=4); (c) Recyclability of P-CMP in real tail liquid (S/L=10g/L, T=298K, 24 h, pH=4).

The design of a two-element simulation system incorporating Nd^{3+} was undertaken for the purpose of conducting selective adsorption experiments, wherein the interfering ions comprised Al^{3+}, Ca^{2+}, Mg^{2+}, Mn^{2+}, K^{+} and Na^{+}. The result was shown in Figure 6a. The presence of Me^{+} and Me^{2+} was no interference to the adsorption of rare earth, and the removal rate of rare earth was above 86%, while less than 3% for impurity ions. Al^{3+} still had an inhibitory effect on the adsorption of rare earth, removed by 56%. The structure of aminophosphoric acid enhances the selectivity of the adsorbent to Me^{+} and Me^{2+}, but the separation of Al^{3+} still needs further investigation.

3.4 Real system

Real rare earth leach tailings were obtained from Changting, Fujian Province. The ion composition of the tailing liquid was shown in Figure 6b. When using 100 mg of adsorbent, the adsorption of rare earth ions in solution was 96.6% while 90% for Al ions, but the adsorption rate of other impurity ions were less than 22%. Al^{3+} and REE^{3+} have similar physical and chemical properties, so they are usually co-adsorbed [10].

3.5 Recyclability

The recyclability of P-CMP was carried out in real system, and 1 M HCl (30ml) was used to desorb the P-CMP at the end of each adsorption. The result after 8 cycles was shown in Figure 6c. After 8 cycles, the adsorption rate of rare earth was still above 80%, and 83% of the original adsorption properties was retained. The results showed that P-CMP had a good cycle stability and cost effectivity.

3.6 Adsorption mechanism

To elucidate the adsorption mechanism, the P-CMP was characterized by X-ray photoelectron spectroscopy (XPS) before and after adsorption. As shown in figure 7 (a), a characteristic peak of Nd^{3+} appeared at binding energy of 1000 eV indicated that the REE^{3+} has been successfully adsorbed by the constructed P-CMP. According to Fig. 7(b), the P fine spectrum is divided into two deconvolution peaks ($2P_{1/2}$ and $2P_{3/2}$). Compared with the original adsorbents, the binding energy of $2P_{1/2}$ decreased from 133.77 to 133.62 eV after adsorption. In addition, according to the O 1s spectrum, the binding energy of P=O and P-OH increased to 531.44 and 532.88 eV, respectively, implying that the phosphate group is strongly coordinated with the Nd^{3+}. Moreover, from the N 1s plot, the binding energy of the primary amine group decreased to 401.58 eV after adsorption, further indicating the synergistic adsorption of REE^{3+} by amino and phosphate groups.

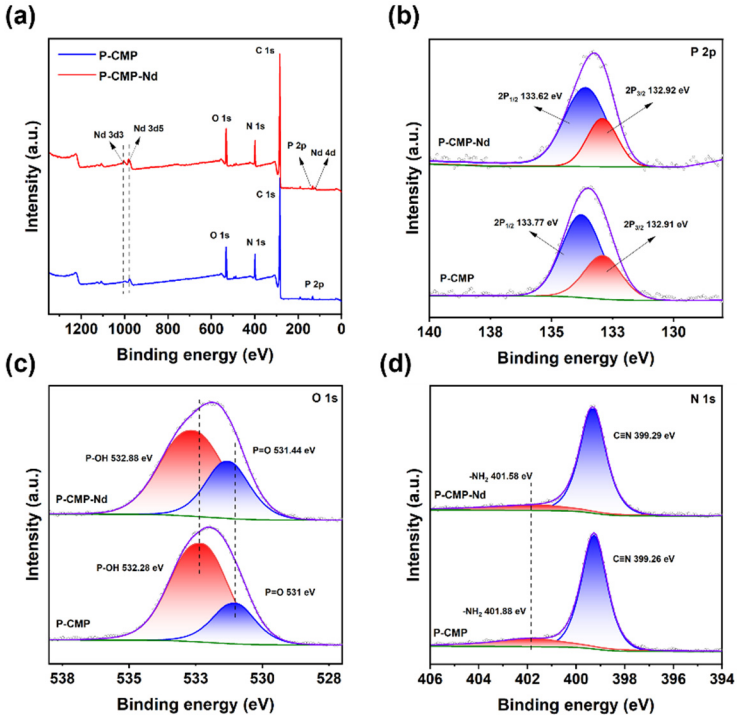

Figure 7. (a) XPS survey spectra of P-CMP; High-resolution N1s (b), O1s(c), and P2p (d) of P-CMP.

4 Conclusion

The present study proposed the utilization of phosphorylated conjugated organic polymer for rare earth enrichment in low-concentration solutions. Furthermore, an investigation was conducted to explore the potential of selective adsorption of rare earth using an aminophosphoric acid structure. Aminophosphoric acid can effectively improve the selectivity of adsorbent to Me^{2+} and Me^{+}. As mentioned above, when the removal rate of rare earth ions reached more than 85%, the removal rate of $Mg^{2+}$and Mn^{2+} could be ignored. The results showed that the optimal adsorption range of pH was 3-7, and the adsorption of P-CMP was monolayer chemisorption. The maximum adsorption capacities of Nd^{3+}, Dy^{3+} and Y^{3+} were 29.79, 38.11 and 27 mg/g, respectively, accompanied by reaching the equilibrium within 20 minutes. P-CMP was used for selective adsorption of rare earth ions in real system and 8 times of cyclic adsorption experiments were carried out, which showed that P-CMP had good selectivity and cyclic stability.

Acknowledgments

The authors gratefully acknowledge financial support from the Jungar Banner applied technology research and development project (2023YY-03) and basic research expenses of universities directly under the Inner Mongolia Autonomous Region (RZ200002361).

References

1. Cheisson, T., and E. J. Schelter (2019) Rare earth elements: Mendeleev's bane, modern marvels. Science, 363: 489-93.
2. Moldoveanu, G. A., and V. G. Papangelakis (2018) An overview of rare-earth recovery by ion-exchange leaching from ion-adsorption clays of various origins. Mineral. Mag., 80: 63-76.
3. Moira Feil， Lukas Rüttinger ， Adelphi, Berlin (2011) Sustainable Prevention of Resource Conflicts: New Risks Raw Materials for the Future? Case Study and Scenarios for China and Rare Earths. Germany Federal Environment Agency, 7: 15-160.
4. Brewer, A., J. Florek, and F. Kleitz (2022) A perspective on developing solid-phase extraction technologies for industrial-scale critical materials recovery. Green Chem., 24: 2752-65.
5. Asadollahzadeh, Mehdi, Rezvan Torkaman, and Meisam Torab-Mostaedi (2020) Extraction and Separation of Rare Earth Elements by Adsorption Approaches: Current Status and Future Trends. Sep. Purif. Reviews, 50: 417-44.
6. Wu, Dongbei, Yawei Gao, Wenjun Li, Xiangning Zheng, YongGui Chen, and Qigang Wang (2016) Selective Adsorption of La^{3+} Using a Tough Alginate-Clay-Poly(n-isopropylacrylamide) Hydrogel with Hierarchical Pores and Reversible Re-Deswelling/Swelling Cycles. ACS Sustainable Chem. Eng., 4: 6732-43.
7. Bi, Shuai, Zhi-An Lan, Silvia Paasch, Wenbei Zhang, Yafei He, Chao Zhang, Feng Liu, Dongqing Wu, Xiaodong Zhuang, Eike Brunner, Xinchen Wang, and

Fan Zhang (2017) Substantial Cyano-Substituted Fully sp^2-Carbon-Linked Framework: Metal-Free Approach and Visible-Light-Driven Hydrogen Evolution. Adv. Funct. Mater., 27.

8. Wu, L., M. Yang, L. Yao, Z. He, J. X. Yu, W. Yin, and R. A. Chi (2022) Polyaminophosphoric Acid-Modified Ion-Imprinted Chitosan Aerogel with Enhanced Antimicrobial Activity for Selective La(III) Recovery and Oil/Water Separation. ACS Appl. Mater. Interfaces, 14: 53947-59.
9. Zhang, Gang, Wenxia Ma, Yuqin Feng, Ming Yang, Zheng Fang, Yongsheng Yang, Weiyan Yin, and Zehao Li (2022) Recyclable Amino-Phosphorylated Polyacrylonitrile Fiber for Gd (III) Adsorption in Aqueous Solution. ACS Appl. Polym. Mater., 4: 8396-406.
10. He, Q., J. F. Chen, L. M. Gan, M. L. Gao, M. M. Zan, and Y. F. Xiao (2023) Insight into leaching of rare earth and aluminum from ion adsorption type rare earth ore: Adsorption and desorption. J. Rare Earths, 41: 1398-407.